NASA TECHNICAL MEMORANDUM

NASA TM X-52190

SOLUTION OF THE BOLTZMANN AND RATE EQUATIONS FOR THE ELECTRON DISTRIBUTION FUNCTION AND STATE POPULATIONS IN NONEQUILIBRIUM MHD PLASMAS

by J. V. Dugan, Jr., F. A. Lyman, and L. U. Albers
Lewis Research Center
Cleveland, Ohio, U.S.A.

TECHNICAL PAPER proposed for presentation at
International Symposium on Magnetohydrodynamic
Electrical Power Generation sponsored by International
Atomic Energy Agency and European Nuclear Energy Agency
Salzburg, Austria, July 4-8, 1966

NATIONAL AERONAUTICS AND SPACE ADMINISTRATION · WASHINGTON, D.C. · 1966

SM-74/191

SOLUTION OF THE BOLTZMANN AND RATE EQUATIONS FOR THE ELECTRON DISTRIBUTION FUNCTION AND STATE POPULATIONS IN NONEQUILIBRIUM MHD PLASMAS

by J. V. Dugan, Jr., F. A. Lyman, and L. U. Albers

Lewis Research Center
Cleveland, Ohio, U. S. A.

TECHNICAL PAPER proposed for presentation at

International Symposium on Magnetohydrodynamic Electrical Power Generation sponsored by International Atomic Energy Agency and European Nuclear Energy Agency
Salzburg, Austria, July 4-8, 1966

NATIONAL AERONAUTICS AND SPACE ADMINISTRATION

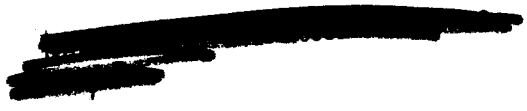

SOLUTION OF THE BOLTZMANN AND RATE EQUATIONS FOR THE ELECTRON DISTRIBUTION FUNCTION AND STATE POPULATIONS IN NONEQUILIBRIUM MHD PLASMAS

J. V. Dugan, Jr., F. A. Lyman, and L. U. Albers

Lewis Research Center
National Aeronautics and Space Administration
Cleveland, Ohio, U.S.A.

REVISED ABSTRACT

Many calculations of the electrical conductivity of nonequilibrium MHD plasmas have been based on a simple two-temperature theory. This theory assumes that (a) the electron number density has the equilibrium (Saha) value corresponding to the electron temperature T_e, and (b) the free electron energy distribution function $f(u)$ is maxwellian.

The validity of assumption (a) has been studied by several authors who, however, used assumption (b) in their analyses. Assumption (b) has been less thoroughly studied. Because both excitation and ionization rates are sensitive to $f(u)$ and bound states may be out of equilibrium due to radiative transitions, it is unrealistic to treat these two assumptions separately. This paper reports preliminary results of an investigation undertaken to establish the range of validity of the two-temperature theory for MHD plasmas by solving the Boltzmann equation for $f(u)$ and the steady-state rate equations for the bound electronic states. The problem was attacked in the following three stages.

First, $f(u)$ was calculated from a Boltzmann equation including only the electric field and the elastic collision terms. The results showed that for typical MHD systems (e.g., Ar + K at 1 atm) electron-electron collisions drive $f(u)$ to maxwellian.

Second, the solution of the rate equations for a maxwellian $f(u)$, using a five-level cesium atomic model, demonstrated the importance of radiative transitions in determining the bound-state populations and magnitudes of the inelastic collision terms. The model atom consisted of four discrete states (6S; 6P,P'; 5D,D'; 7S) and a lumped state, which was assigned various binding energies and degeneracies. Criteria for selecting the latter were based on the maximum stable orbit radius that would be likely for the plasmas of interest. Both the classical Bohr-

Thomson and Gryzinski cross sections were used to calculate the rate coefficients and collision terms for excitation, deexcitation, ionization, and three-body capture. Many calculations were also performed using recent experimental data for the 6S → 6P,P' excitation. Known values of radiative probabilities were used for transitions between discrete states.

Finally, the simultaneous solution of the Boltzmann equation (including all relevant elastic and inelastic collision terms) and the bound-state rate equations was attempted by an iterative technique. Plasmas of various optical thicknesses to resonance radiation were considered. In the extreme case of a gas transparent to all line radiation, the departure of the state populations from equilibrium causes a large reduction in the free electron number density, especially at low values of T_e. Because excitation collisions are not balanced by superelastic collisions in this case, they cause f(u) to depart significantly from maxwellian at high energies. Numerical difficulty was encountered in the iterative scheme in this case. The effect of inelastic collisions is much less pronounced for plasmas that are optically thick to resonance radiation, and it disappears altogether for a plasma optically thick to all radiation. The distribution function was calculated for a range of electric fields and gas densities for the case where resonance radiation is completely trapped, the most realistic situation for large MHD generators. The dependence of the electrical conductivity on the current density was also calculated, and where possible compared with experimental results.

SOLUTION OF THE BOLTZMANN AND RATE EQUATIONS FOR THE ELECTRON DISTRIBUTION FUNCTION AND STATE POPULATIONS IN NONEQUILIBRIUM MHD PLASMAS

J. V. Dugan, Jr., F. A. Lyman, and L. U. Albers

Lewis Research Center
National Aeronautics and Space Administration
Cleveland, Ohio, U.S.A.

INTRODUCTION

A fundamental problem of gas discharge theory is the prediction of the free electron number density and velocity distribution function, which together determine the electrical properties of the gas. In the case of certain low-voltage atmospheric-pressure glow discharges in alkali-seeded noble gases, which are being studied for nonequilibrium magnetohydrodynamic (MHD) power generation, this problem is fortunately somewhat alleviated. For such discharges, a simple two-temperature conduction theory due to Kerrebrock [1] has shown reasonable agreement with experiment at sufficiently high current densities (above 10^4 amps-m^{-2}). Kerrebrock's theory assumes that (a) the free electron energy distribution $f(u)$ is maxwellian, with a temperature T_e that may considerably exceed the gas temperature T_g, and (b) the free electron number density N_e is given by the Saha equation applied at temperature T_e.

There remains, however, the question of the range of validity of the two-temperature theory. Kerrebrock and Hoffman [2] attributed the lack of agreement between theory and experiment at low current densities (below 3×10^3 amps-m^{-2}) to the fact that electron-electron collisions could not preserve a maxwellian velocity distribution in the presence of elastic electron-atom collisions, due to the low value of N_e. They supported their hypothesis by estimating average frequencies of energy transfer through these collisions.

Archambault and Cuenca [3], on the other hand, concluded that the distribution function would be maxwellian under MHD conditions. This conclusion was based on a detailed comparison of the various elastic and inelastic collision frequencies in an argon-cesium plasma, unfortunately for only one set of values of N_e, T_e, T_g, and argon and cesium number densities. The authors of [3] raised doubts concerning the validity of the Saha equation, however - a position which is contrary to the conclusions

of an earlier study by Ben Daniel and Tamor [4].

The present work attempts to ascertain the validity of the two-temperature theory for alkali-seeded argon MHD plasmas by calculating $f(u)$ and N_e self-consistently from the Boltzmann and rate equations. Such a self-consistent calculation is necessitated by the fact that $f(u)$ depends strongly on N_e [5], which in turn is very sensitive to the behavior of $f(u)$ above the excitation and ionization thresholds [6].

THEORY

Electron Boltzmann equation

The energy distribution function[1] $f(u)$ is defined such that $u^{1/2}f(u)du$ is the fraction of electrons having energies in the range from u to $u + du$ electron volts; hence,

$$\int_0^\infty u^{1/2}f(u)du = 1 \tag{1}$$

For a steady-state discharge in a uniform, partially ionized gas flowing through crossed electric and magnetic fields, the appropriate equation for $f(u)$ is[2] [5,7,8]

$$\underbrace{\frac{(E^*)^2}{3}\frac{\lambda(u)}{1+\omega^2\tau^2}u\frac{df}{du}}_{\text{(i)}} + \underbrace{\sum_{h=a,i}\frac{2m_e}{m_h}u^2N_hQ_{eh}^m(u)\left[f(u)+\frac{kT_g}{e}\frac{df}{du}\right]}_{\text{(ii)}}$$

$$+ \underbrace{\frac{1}{2}N_eu^2Q_{ee}^m(u)\left\{\frac{df}{du}\left[\frac{2}{3}\int_0^u (u')^{3/2}f(u')du' + \frac{2}{3}u^{3/2}\int_u^\infty f(u')du'\right]\right.}_{\text{(iii)}}$$

$$\underbrace{\left. + f(u)\int_0^u (u')^{1/2}f(u')du'\right\}}_{\text{(iv)}} = I(f) \tag{2}$$

Equation (2) is sometimes called the gain equation, because when multiplied by $N_e(2e/m_e)^{1/2}$ its terms give the rates (in m^{-3}-sec^{-1}) at which electrons are added to (or lost from) the energy range u to ∞. The terms are as follows:

(i) Energy gain from the effective electric field $\vec{E}^*$

---

[1] Strictly speaking, $u^{1/2}f(u)$ is the energy distribution function, but the above terminology will be used for brevity.

[2] Symbols are defined in appendix A.

(ii) Energy loss to atoms and ions in elastic collisions

(iii) Energy exchange in electron-electron collisions

(iv) Energy gain (loss) in inelastic (including superelastic) collisions with atoms and ions

The inelastic gain term $I(f)$ is the sum of the following expressions obtained by integrating the inelastic collision terms given in [8,9] from u to ∞, making simple transformations, and using the microscopic reversibility relation between excitation and deexcitation cross sections (Klein-Rosseland relation) and between ionization and three-body capture cross sections [9]:

(a) Excitation and deexcitation by electron impact

$$I_{ex+dex}(f) = -\sum_{L,K>L} \int_{u}^{u+\Delta E_{L,K}} \left[N_L f(u') - \frac{g_L}{g_K} N_K f(u' - \Delta E_{L,K}) \right] \times u' Q^{ex}_{L\to K}(u') du' \qquad (3)$$

(b) Ionization by electron impact

$$I_{ion}(f) = \sum_{L} N_L \left\{ \int_{u+E_L}^{\infty} u' f(u') du' \int_{u}^{u'-E_L} \left[\sigma^{ion}_L(u'',u') + \sigma^{ion}_L(u' - u'' - E_L,u') \right] du'' - \int_{u}^{\infty} u' f(u') du' \int_{0}^{u'-E_L} \sigma^{ion}_L(u'',u') du'' \right\} \qquad (4)$$

(c) Three-body ion-electron-electron capture[3]

$$I_{cap}(f) = \frac{\sqrt{\pi}}{2}\left(\frac{h^2}{2\pi m_e e}\right)^{3/2} N_e N_i \sum_{L} \frac{g_L}{2g_i} \left\{ \int_{u}^{\infty} u' du' \int_{0}^{u'-E_L} f(u'') f(u' - u'' - E_L) \times \sigma^{ion}_L(u'',u') du'' - \int_{u+E_L}^{\infty} u' du' \int_{u}^{u'-E_L} f(u'') f(u' - u'' - E_L) \left[\sigma^{ion}_L(u'',u') + \sigma^{ion}_L(u' - u'' - E_L,u') \right] du'' \right\} \qquad (5)$$

[3]Three-body collisions in which the third body is an atom or ion will not be considered.

(d) Radiative capture[4]

$$I_{r\text{-}cap}(f) = -N_i \sum_L \int_u^\infty u' f(u') \sigma_L^{r\text{-}cap}(u') du' \tag{6}$$

When $u = 0$, the excitation-deexcitation term (3) vanishes because $Q^{ex}_{L\to K}(u) = 0$ for $u \le \Delta E_{L,K}$, while the terms (4), (5), and (6), when multiplied by $N_e(2e/m_e)^{1/2}$, become the total ionization and capture rates. Also, when the bound and free electrons are in equilibrium, the term (3) vanishes while (4) and (5) cancel.

Rate equations for bound electrons

The rate of change of the number of bound electrons in level L is

$$\dot{N}_L = -N_L(N_e \mathcal{K}_L + \mathcal{A}_L) + N_e \sum_{K \neq L} N_K K_{K\to L} + \sum_{K>L} N_K A_{K\to L} + N_e N_i \left(K_L^{cap} + \beta_L\right) \tag{7}$$

For the steady-state problem treated herein, $\dot{N}_L = 0$. Equation (7) together with the normalization condition

$$N_i + \sum_L N_L = N_s^0 \tag{8}$$

and the condition of charge neutrality ($N_e = N_i$) serve to determine N_e and N_L for a specified $f(u)$ and initial seed number density N_s^0.

Electrical conductivity

The electron current density $\vec{j}$ in the plane perpendicular to $\vec{B}$ is [7]

$$\vec{j} = \sigma_\perp \vec{E}^* + \sigma_H \frac{\vec{B}}{B} \times \vec{E}^* \tag{9}$$

where

$$\sigma_\perp = \frac{1}{3} N_e e \left(\frac{2e}{m_e}\right)^{1/2} \int_0^\infty \frac{1}{1 + \omega^2\tau^2} \lambda(u) u \left(-\frac{df}{du}\right) du \tag{10}$$

$$\sigma_H = \frac{1}{3} N_e e \left(\frac{2e}{m_e}\right)^{1/2} \int_0^\infty \frac{\omega\tau}{1 + \omega^2\tau^2} \lambda(u) u \left(-\frac{df}{du}\right) du \tag{11}$$

are the perpendicular and Hall conductivities, respectively.

[4]The inverse process to (d), photoionization, is ignored.

Electron energy equation

The electron energy balance equation may be derived from equation (2) by multiplying by $N_e e(2e/m_e)^{1/2}$ and integrating from $u = 0$ to ∞. After considerable transformation, the result may be written as

$$\vec{j} \cdot \vec{E}^* = N_e e \left\{ \left(\frac{2e}{m_e}\right)^{1/2} \sum_{h=a,i} \frac{2m_e}{m_h} N_h \int_0^\infty u^2 Q_{eh}^m(u) \left(f(u) + \frac{kT_g}{e} \frac{df}{du} \right) du \right.$$

$$+ \sum_{L,K>L} \Delta E_{L,K} (N_L K_{L\to K} - N_K K_{K\to L}) + \sum_L E_L \left(N_L K_L^{ion} - N_i K_L^{cap} \right)$$

$$\left. + \left(\frac{2e}{m_e}\right)^{1/2} N_i \sum_L \int_0^\infty u^2 f(u) \sigma_L^{r\text{-}cap}(u) du \right\} \left(\frac{W}{m^3}\right) \qquad (12)$$

Equation (12) can, of course, also be derived from elementary considerations. By multiplying equation (7) by E_L and summing over all bound levels L, one can show that the inelastic terms in (12) (the last three on the right) are equal to the power loss per unit volume through line and continuum radiation; that is,

$$W_R \equiv \sum_{L,K<L} e\, \Delta E_{K,L} N_L A_{L\to K} + N_e N_i e \left(\frac{2e}{m_e}\right)^{1/2} \sum_L \int_0^\infty (E_L + u) u f(u) \sigma_L^{r\text{-}cap}(u) du \left(\frac{W}{m^3}\right) \qquad (13)$$

For a maxwellian $f(u)$, the elastic loss term (the first on the right of (12)) is proportional to the temperature difference $T_e - T_g$, and equation (12) provides a means of calculating T_e. If $f(u)$ is not maxwellian, the temperature can be determined from the relation

$$\frac{kT_e}{e} = \frac{2}{3} \int_0^\infty u^{3/2} f(u) du \qquad (14)$$

CALCULATIONS AND RESULTS

Computational procedure

An iterative technique was employed to solve equations (2) and (7). The coefficients of the rate equations (7) are first calculated for an assumed $f(u)$ (usually a maxwellian with a guessed T_e). Solution of these equations yields N_e and N_L. When these number densities and the assumed $f(u)$ are used, the inelastic term $I(f)$ and the integrals in the electron-electron collision term are then calculable. This reduces the equation for the next approximation to a first-order linear differential equation in $f(u)$, which is integrated numerically. The solution is then normalized to satisfy equation (1) and an electron temperature calculated from equation (14). When $f(u)$ is very close to maxwellian, equation (14) becomes an identity, and it is necessary to determine T_e by satisfying

the energy equation (12). Otherwise, the process is repeated until convergence is obtained in $f(u)$, T_e, and N_e.

Results of elastic-collision problem

Initial calculations were concerned with determining $f(u)$ from equation (2), neglecting the inelastic term $I(f)$. These calculations were performed for argon seeded with potassium and cesium under the conditions of Kerrebrock and Hoffman's experiment, to see whether a non-maxwellian distribution would be obtained at low current densities, as hypothesized in [2]. For these calculations there was no magnetic field, and N_e was assumed to be given by the Saha equation. Elastic cross sections for argon, potassium, and cesium were taken from [10, 11, 12], respectively.

It was found that $f(u)$ is maxwellian over the entire range of current densities measured in [2]. The computed electrical conductivity is plotted as a function of current density in figure 1 along with Kerrebrock and Hoffman's data. The lowest calculated value of N_e was 3×10^{18} m^{-3}, as noted on the figure, whereas Kerrebrock and Hoffman estimated that electron-electron collisions could not maintain a maxwellian $f(u)$ if N_e were below 3×10^{19} m^{-3}. Neither the present theory nor Kerrebrock's theory shows the dip in conductivity observed at 10^3 amp-m^{-2}.

Cesium atomic model

For investigation of the effect of inelastic collisions, a five-level model cesium atom, which contained three discrete excited states, was chosen. These states (6P, P'; 5D, D'; 7S) were treated as singlets, neglecting the slight splitting of the 6P and 5D states due to spin-orbit coupling. All the remaining excited states of cesium were collapsed into a lumped state whose degeneracy and binding energy were varied to explore the sensitivity of the calculation to this atomic model. Various criteria were employed to estimate the maximum stable electronic orbit radius. The features of the atomic model are summarized in Table I.

Inelastic cross sections for electron-cesium atom collisions

(a) Excitation-deexcitation

Experimental [13,14] and theoretical [15,16] curves for the first (6S → 6P) and total excitation cross sections of cesium are shown in figure 2. In computations the experimental [13] curve was used above 2 eV, with a linear segment of slope 71 Å^2 - eV^{-1} [14] for $1.42 \leq u \leq 2$ eV.

The conventional Gryzinski cross sections [16] were used for the remaining optically allowed transitions, and the Gryzinski exchange formula [17] was used for optically forbidden transitions. The classical Bohr-Thomson cross sections [9] provided a check on the accuracy of the computations, since their use enables analytical evaluation of the collision terms for a maxwellian $f(u)$.

(b) Ionization-capture

The Gryzinski ionization cross sections [16] were employed for transi-

tions from all bound electronic states to the continuum. The maximum cross section predicted for ionization from the ground (6S) state is 20 percent lower than the best experimental value [18].

Radiative transitions

(a) Deexcitation

The radiative transition probabilities listed in Table I were taken from [19]. The optical thickness of the plasma can be varied simply by altering these values, thus simulating different plasma dimensions and optical absorption coefficients.

(b) Radiative capture

At low N_e and T_e, radiative capture becomes important. Cross sections for this process were taken from [20].

Solution of rate equations for maxwellian distribution

Figures 3 and 4 show the results of solving the steady-state rate equations (7) for a maxwellian f(u). In figure 3 the degree of ionization of the cesium is plotted as a function of the initial cesium number density N^o_{Cs} for $kT_e/e = 0.2$ eV. The results are qualitatively similar to those of [4]. For an optically thin plasma, N_e is determined at very low N^o_{Cs} by the balance between radiative capture and collisional ionization from the ground state. With increasing N^o_{Cs}, three-body capture becomes important, and in the optically thin case, the curve rises to a maximum as ionization from excited states becomes significant, thereafter approaching the Saha curve. For a plasma optically thick to resonance radiation, ionization from excited states is important at lower N^o_{Cs} because the populations of these states are higher. Figure 3 also demonstrates the relative insensitivity of the results to the degeneracy and binding energy of the lumped state.

Figure 4 shows that the Saha equation is a good approximation when $T_e \gtrsim 3000^o$ K, regardless of the optical thickness of the plasma. Below this temperature, the optical thickness of the plasma to resonance radiation is the controlling factor in determining the magnitude of the inelastic term I(f). When resonance radiation completely escapes, the lack of detailed balancing of collisional transitions between the 6S and 6P states results in a large (negative) contribution to I(f), which is comparable in magnitude to the electron-electron collision term. For a plasma optically thick to resonance radiation, collisional transitions between these states are more nearly in balance, and I(f) is an order of magnitude smaller and due mainly to the 6P → 5D and 5D → 7S transitions.

Distribution function and electrical conductivity - inelastic case

Preliminary results obtained by iterative solution of equations (2) and (7) are shown in figures 5 and 6 for an atmospheric-pressure argon-cesium plasma optically thick to resonance radiation, the most realistic case for an MHD generator [21]. These calculations were performed for a seed fraction $\left(N^o_{Cs}/N_{Ar}\right)$ of 0.0015, gas temperature of 1500° K, and no

magnetic field, as in the experiments of [2]. The conductivity - current curve of figure 5 displays the same general features as the experimental argon-potassium results. Of particular interest is the fact that the theoretical curve drops off more rapidly with decreasing current than in the elastic case. The reason is that the states are out of equilibrium at low currents and electron temperatures, and there is an appreciable inelastic energy loss from the electrons, as well as a sizable reduction of N_e below the Saha value. At the higher values of j, the two-temperature theory is a good approximation, as shown by the distribution function plot of figure 6 where the calculated f(u) at $T_e = 3000^\circ$ K is indistinguishable from a maxwellian. At 2000° K, however, f(u) departs from maxwellian above the first excitation potential. Since convergence difficulties were encountered for $T_e < 2300^\circ$ K, the results in this range are uncertain, and their questionable nature is indicated by the dashed portion of the theoretical curve in figure 5. In the optically thin case, convergence difficulties were experienced at even higher values of T_e.

Conclusions

(a) Elastic collisions cannot alone account for anomalies in the electrical conductivity observed at low current densities.

(b) The Saha equation is a good approximation when either the cesium number density is above 10^{24} m^{-3} or the electron temperature above 3000° K, regardless of the optical thickness of the plasma. At lower densities or temperatures, the optical thickness to resonance radiation controls the electron number density and the magnitude of the inelastic collision terms. Fortunately, the electron number density proves to be relatively insensitive to the assumptions made concerning the lumped state.

(c) Preliminary results of a self-consistent calculation of the electron number density and distribution function show trends that agree with available experimental data, but more work is required to obtain reliable results at low electron temperatures, where inelastic effects dominate.

REFERENCES

[1] KERREBROCK, J. L., "Conduction in gases with elevated electron temperature," Engineering Aspects of Magnetohydrodynamics (MANNAL, C., MATHER, N. W., Eds.), Columbia Univ. Press, New York (1962) 327.

[2] KERREBROCK, J. L., HOFFMAN, M. A., Nonequilibrium ionization due to electron heating: II. Experiments, AIAA J. 2 (1964) 1080.

[3] ARCHAMBAULT, Y., CUENCA, N., Fonction de distribution et densite electronique d'un plasma hors d'equilibre thermodynamique, Proc. Int. Symposium MHD Elec. Power Generation, Vol. 1, Paris (1964) 349; Discussion, Vol. 4 (1964) 1793.

[4] BEN DANIEL, D. J., TAMOR, S., Nonequilibrium ionization in magnetohydrodynamic generators, Rept. 62-RL-(2922-E), General Electric Research Lab (1962).

[5] DREICER, H., Electron velocity distributions in a partially ionized gas, Phys. Rev. 117 (1960) 343.

[6] DEWAN, E. M., Generalizations of the Saha equation, Phys. Fluids 4 (1961) 759.

[7] ALLIS, W. P., Motions of ions and electrons, Handbuch der Physik (FLÜGGE, S., Ed.), Vol. XXI, Springer-Verlag, Berlin (1956) 383.

[8] HOLSTEIN, T., Energy distribution of electrons in high frequency gas discharges, Phys. Rev. 70 (1946) 367.

[9] FOWLER, R. H., Statistical Mechanics, 2nd ed., Cambridge Univ. Press (1936) 17.4, 17.6.

[10] FROST, L. S., PHELPS, A. V., Momentum-transfer cross sections for slow electrons in He, Ar, Kr, and Xe from transport coefficients, Phys. Rev. 136 (1964) A1538.

[11] BRODE, R. B., The absorption coefficient for slow electrons in alkali metal vapors, Phys. Rev. 34 (1929) 673.

[12] CROWN, J. C., RUSSEK, A., Electron-alkali-atom interaction potential and elastic-scattering cross section, Phys. Rev. 138 (1965) A669.

[13] ZAPESOCHNY, I. P., SHIMON, L. L., Absolute excitation cross sections of the alkali metals, IVth Int. Conf. on the Physics of Electronic and Atomic Collisions, Science Bookcrafters, Inc., Hastings-on-Hudson, New York (1965) 401.

[14] NOLAN, J. F., EMMERICH, W. S., Electron collision cross sections in metal vapors, Rept. No. 1E5-MHDIN-R1, Westinghouse Electric Co. (NASA CR-54474) (1965).

[15] HANSEN, L. K., Cross section of the electron-induced 6s-6p transition in cesium, J. Appl. Phys. 35 (1964) 254.

[16] GRYZINSKI, M., Classical theory of electronic and ionic inelastic collisions, Phys. Rev. 115 (1959) 374.

[17] GRYZINSKI, M., Classical theory of atomic collisions. I. Theory of inelastic collisions, Phys. Rev. 138 (1965) A336.

[18] SHELDON, J. W., DUGAN, J. V., Jr., Semiclassical calculation of inelastic cross sections for electron-cesium atomic collisions, J. Appl. Phys. 36 (1965) 650.

[19] ROBERTS, T. G., HALES, W. L., Radiative transition probabilities and absorption oscillator strengths for the alkali-like ions of the alkaline earths and for calcium I, Rept. AMC-RR-TR-62-8, Redstone Arsenal (1962).

[20] NORCROSS, D. W., STONE, P. M., Radiative recombination in cesium, Rept. SRRC-RR-65-95, Sperry Rand Res. Center (1965).

[21] BYRON, S., BORTZ, P. I., RUSSELL, G. R., Electron-ion reaction rate theory: Determination of the properties of nonequilibrium monatomic plasmas in MHD generators and accelerators and in shock tubes, Proc. 4th Symposium on the Engineering Aspects of Magnetohydrodynamics (1963) 93.

APPENDIX A - SYMBOLS[5]

$A_{L\to K}$ probability (sec^{-1}) of spontaneous radiative transition L→K

$\mathcal{A}_L \equiv \sum_{K<L} A_{L\to K}$

$\vec{B}$ magnetic field

$\vec{E}$ electric field

$\vec{E}^* \equiv \vec{E} + \vec{U} \times \vec{B}$, effective electric field

E_L binding energy of level L, eV

$\Delta E_{L,K} \equiv E_L - E_K$

e electron charge

f(u) energy distribution function (cf. footnote 1)

g degeneracy

h Planck constant

I(f) inelastic gain

j current density

$K_{L\to K} = (2e/m_e)^{1/2} \int_0^\infty uf(u) \times Q_{L\to K}(u)du$, rate coefficient ($m^3$ - sec^{-1}) for collision-induced transition L→K

$K_L^{cap} = (2e/m_e)N_e \int_0^\infty \int_0^\infty uf(u)u'f(u') \times \sigma_L^{cap}(u',u)du'du$, effective two-body rate coefficient (m^3 - sec^{-1}) for capture into level L

$K_L^{ion} = (2e/m_e)^{1/2} \int_{E_L}^\infty uf(u) \times Q_L^{ion}(u)du$, rate coefficient for ionization from level L

$\mathcal{K}_L \equiv \sum_K K_{L\to K} + K_L^{ion}$

k Boltzmann constant

m particle mass

N number density

$Q_{ee}^m(u) = 4Q_{ei}^m(u) = 4\pi(e/4\pi\epsilon_o)^2 u^{-2} \ln \Lambda$

$Q_{ej}^m(u)$ cross section for momentum transfer between electrons and species j (j = a,e,i)

$Q_{L\to K}(u)$ total cross section for collision-induced transition L→K

$Q_L^{ion}(u) = \int_0^{u-E_L} \sigma_L^{ion}(u",u)du"$, total cross section for ionization from level L

T temperature

$\vec{U}$ gas velocity

u electron energy ($m_e v^2/2e$), eV

v electron speed

W_R radiative power loss per unit volume

[5]Mks units are used for all quantities

β_L	rate coefficient (m^3-sec^{-1}) for radiative capture into level L
ϵ_o	permittivity of vacuum
Λ	$= 12\pi(\epsilon_o kT_e)^{3/2}e^{-3}N_e^{-1/2}$, ratio of Debye radius to impact parameter for 90° scattering
$\lambda(u)$	$\equiv \left[\sum_{h=a,i} N_h Q_{eh}^m(u)\right]^{-1}$, free path for elastically scattered electron
σ	electrical conductivity
$\sigma_L^{cap}(u',u)$	probability (m^4-sec) for capture of u'-electron into level L, with u-electron gaining excess energy $u' + E_L$
$\sigma_L^{ion}(u'',u')$	differential cross section (m^2-eV^{-1}) for producing a u" secondary electron by impact of a u' primary electron
τ	$= \lambda(u)/v$, collision time
ω	$\equiv eB/m_e$, electron cyclotron frequency

Subscripts and superscripts:

Ar	argon
a	atom
Cs	cesium
cap	capture
dex	deexcitation
e	electron
ex	excitation
g	gas
H	Hall
h	heavy particle (atom or ion)
i	ion
ion	ionization
K	potassium
K,L	atomic level indices
r-cap	radiative capture
s	seed
0	initial number density
$\perp$	perpendicular

TABLE I. - PARAMETERS OF CESIUM ATOMIC MODEL

State	Level L	Binding energy, E_L, eV	Degeneracy, g_L	Radiative transition probability, $A_{K \to L}$, 10^7 sec^{-1}				
				K = 1	K = 2	K = 3	K = 4	K = 5
6S	1	3.89	2	-----	6.10[c]	----[d]	----[d]	0.306[c]
6P,P'	2	2.47	6	-----	-----	0.178	1.76	.564
5D,D'	3	2.09	10	-----	-----	-----	----[d]	.378
7S	4	1.59	2	-----	-----	-----	-----	.849
Lumped	5	Varied[a]	Varied[b]	-----	-----	-----	-----	----

[a] E_5 = 0.4, 0.6, 0.8 eV.

[b] g_5 = 50, 100, 150.

[c] For plasmas optically thick to resonance radiation, these are equated to zero.

[d] Forbidden transition ($\Delta l \neq \pm 1$).

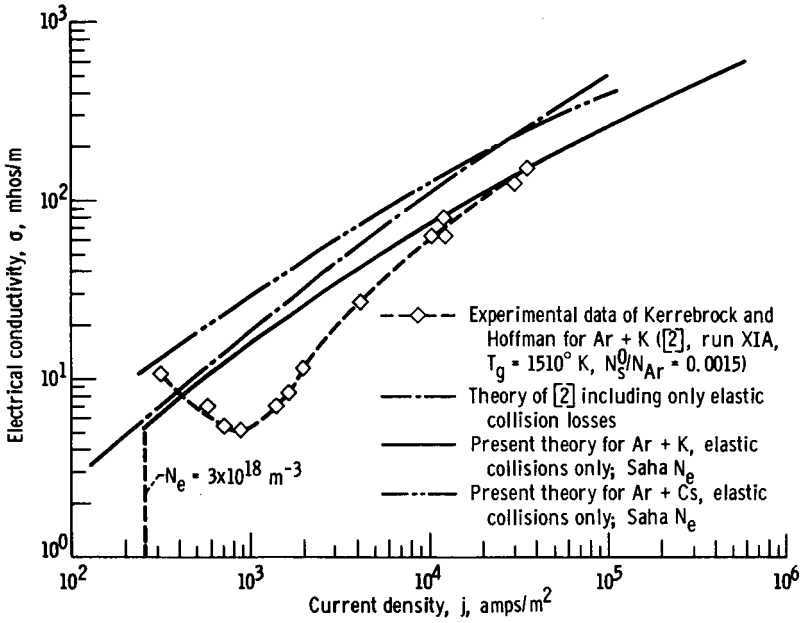

Figure 1. - Comparison of present theory with theoretical and experimental results of Kerrebrock and Hoffman [2]. Gas temperature, 1500° K; seed fraction, N_s^0/N_{Ar}, 0.0015.

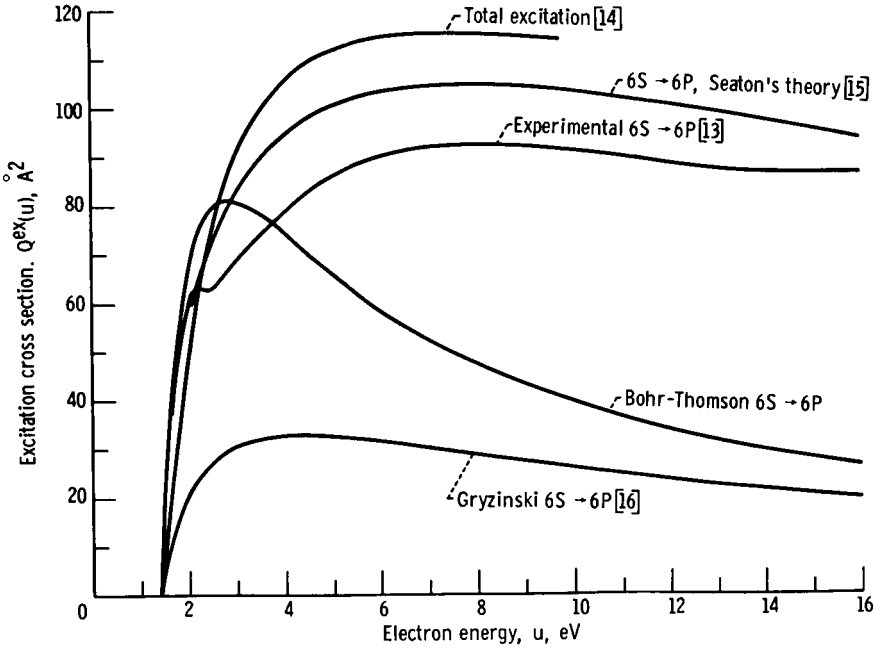

Figure 2. - Excitation cross sections for cesium.

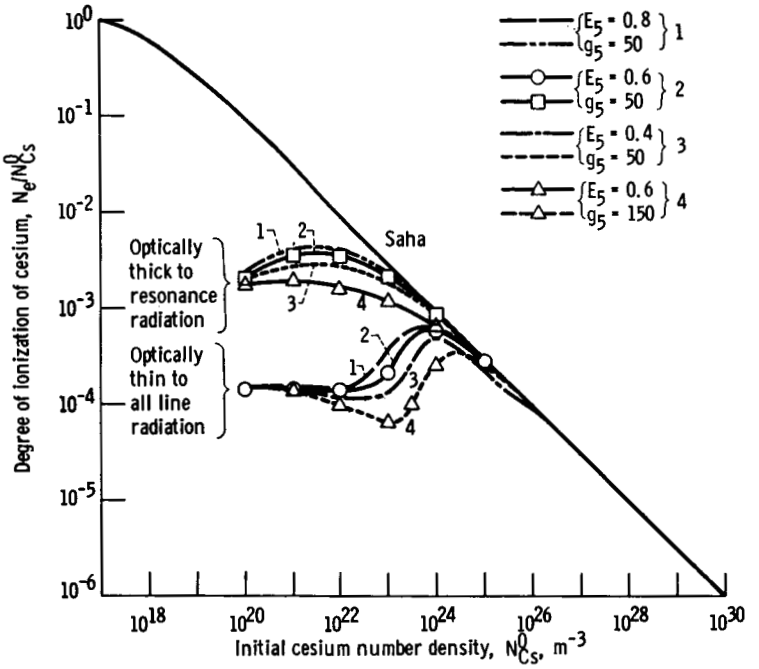

Figure 3. - Degree of ionization of cesium as function of initial seed number density. kT_e/e, 0.2 eV.

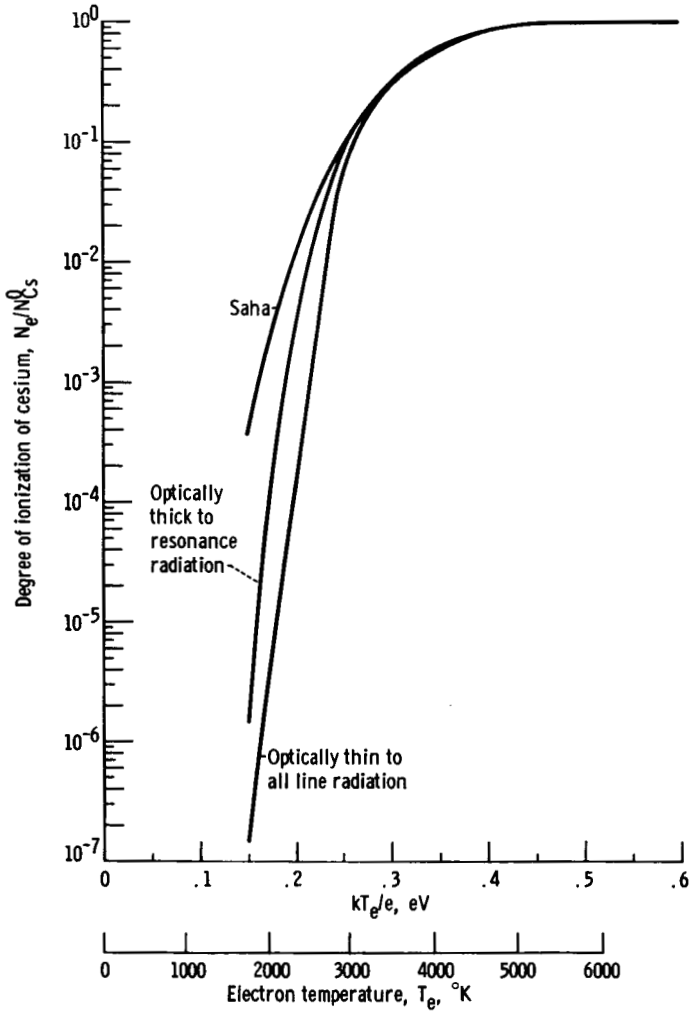

Figure 4. - Degree of ionization of cesium as function of electron temperature. Atmospheric pressure; gas temperature, 1500° K; seed fraction, 0.0015 (N_{Ar} = 4.89x10^{24} m^{-3}, N^0_{Cs} = 7.34x10^{21} m^{-3}).

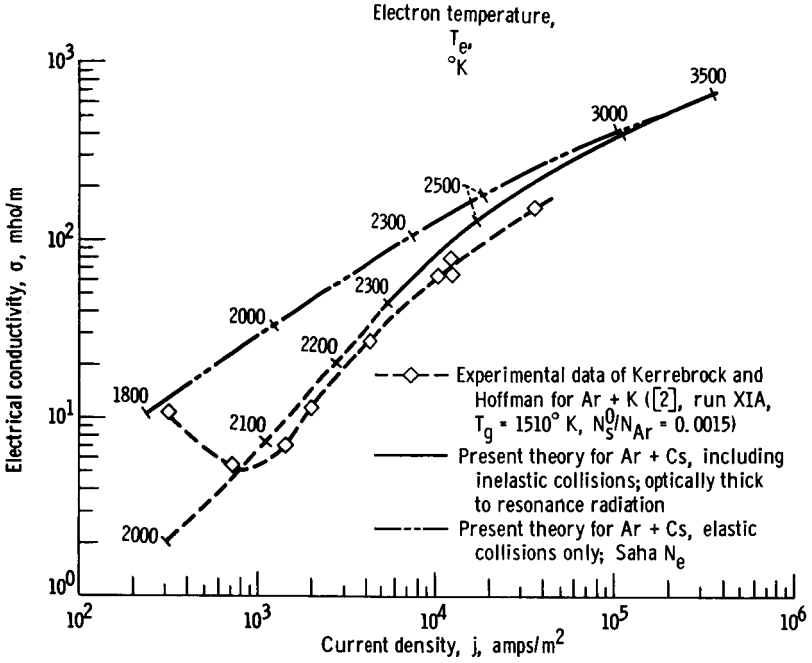

Figure 5. - Electrical conductivity as function of current density. Atmospheric pressure; gas temperature, 1500° K; seed fraction, 0.0015.

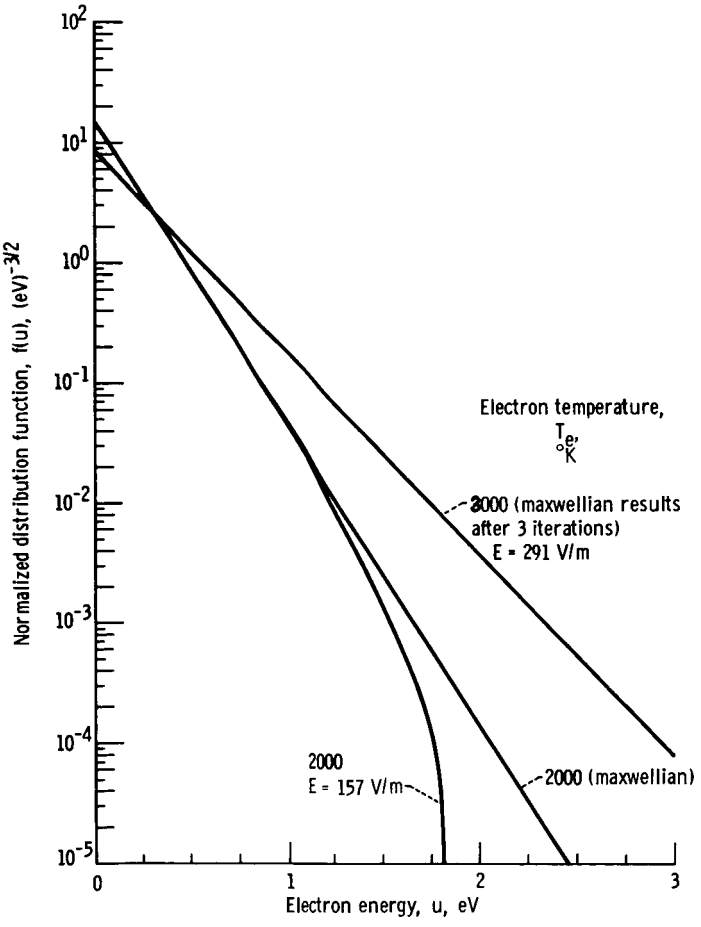

Figure 6. - Normalized distribution function. Argon seeded with cesium; atmospheric pressure; gas temperature, 1500° K; seed fraction, 0.0015; optically thick to resonance radiation.